Heliyon 10 (2024) e29901

Contents lists available at ScienceDirect

Heliyon

journal homepage: www.cell.com/heliyon

Research article

CPE correlates with poor prognosis in gastric cancer by promoting tumourigenesis

Jiarui Lin [a,1], Chengzhi Huang [a,b,c,1], Wenfei Diao [a,d], Haoming Liu [a], Hesong Lu [e], Shengchao Huang [a], Junjiang Wang [a,*]

[a] Department of Gastrointestinal Surgery, Department of General Surgery, Guangdong Provincial People's Hospital (Guangdong Academy of Medical Sciences), Southern Medical University, Guangzhou, 510080, China
[b] Department of General Surgery, Guangdong Provincial People's Hospital Ganzhou Hospital (Ganzhou Municipal Hospital), Ganzhou, 341000, China
[c] School of Medicine, South China University of Technology, Guangzhou, 510006, China
[d] Shantou University Medical College, Shantou, 515000, China
[e] Guangdong Cardiovascular Institute, Guangdong Provincial People's Hospital, Guangdong Academy of Medical Sciences, 510080, China

ARTICLE INFO

Keywords:
CPE
Tumourigenesis
Gastric cancer
Nomogram
Immune cell infiltration
Erk/Wnt pathways
Epithelial-mesenchymal transition

ABSTRACT

Aims: To investigate the potential functions and mechanisms of tumourigenesis in carboxypeptidase E (CPE) and its prognostic value in gastric cancer, and to develop a predictive model for prognosis based on CPE.
Results: Transcriptome level variation and the prognostic value of CPE in different types of cancers were investigated using bioinformatics analyses. The association between CPE and clinicopathological characteristics was specifically explored in gastric cancer. Elevated CPE expression was associated with poor survival and recurrence prognosis and was found in cases with a later clinical stage of gastric cancer. The CPE was considered an independent prognostic factor, as assessed using Cox regression analysis. The prognostic value of CPE was further verified through immunohistochemistry and haematoxylin staining. Enrichment analysis provided a preliminary confirmation of the potential functions and mechanisms of CPE. Immune cell infiltration analysis revealed a significant correlation between CPE and macrophage infiltration. Eventually, a prognosis prediction nomogram model based on CPE was developed.
Conclusion: CPE was identified as an independent biomarker associated with poor prognosis in gastric cancer. This suggests that CPE overexpression promoted epithelial-mesenchymal transition via the activation of the Erk/Wnt pathways, leading to proliferation, invasion, and metastasis. Targeted therapeutic strategies for gastric cancer may benefit from these findings.

1. Introduction

Gastric cancer (GC) is the sixth most prevalent type of cancer worldwide. In 2020, GC accounted for 7.7 % of all cancer-related fatalities and 5.6 % of all cancer-related diagnoses [1]. After understanding the underlying mechanisms, molecular biomarkers can be used for prognosis prediction and evaluation of therapeutic responses in clinical practice, providing valuable therapeutic strategies

* Corresponding author.
E-mail address: wangjunjiang@gdph.org.cn (J. Wang).
[1] These authors contributed equally to this work.

https://doi.org/10.1016/j.heliyon.2024.e29901
Received 4 December 2023; Received in revised form 16 April 2024; Accepted 17 April 2024
Available online 18 April 2024

to inhibit tumour cell formation and progression [2].

Carboxypeptidase E (CPE), a member of the metallocarboxypeptidase gene family, is located on human chromosome 4q32.3 [3,4]. CPE was initially identified as a prohormone-processing enzyme with an exopeptidase function that can produce peptide hormones and neuropeptides in the central nervous and endocrine systems by cleaving amino acid residues at the C-terminal domains [5,6]. CPE is also associated with many metabolic disorders in the human body, including infertility, diabetes mellitus, obesity, glucose homeostasis, and bone remodelling. It also plays a crucial role in psychiatric and mental processes, including emotional responses, memory, and Alzheimer's disease [3,7–10].

CPE can modulate tumour cell proliferation and apoptosis, especially in hypoxic environments, presenting prognostic value in various kinds of cancers [11]. It can stimulate tumourigenesis and pelvic lymph node metastasis, particularly in early-stage cervical cancer and colorectal cancer (CRC) [12–14]. Overexpression of CPE can significantly shorten the interval of tumour relapse and is correlated with poor survival of patients at all stages of lung adenocarcinoma [15,16]. CPE is a substantial prognostic marker in CRC cell lines and primary cancer tissues, which can upregulate the quantity and velocity of cell proliferation and tumourigenic activity [17]. CPE is associated with longer survival of tumour cells under hypoxic and nutrient-starved conditions in hepatocarcinoma and pheochromocytoma. In addition, downregulation of CPE expression inhibits cell migration and invasion in fibrosarcoma and pancreatic cancer, which can also increase resistance to cisplatin in pancreatic cancer [18–20]. Furthermore, downregulation of CPE expression inhibits tumour cell proliferation and migratory capabilities, with a notable decrease in the expression levels of cyclin D-1, leading to cell cycle arrest at the G(0)/G(1) phase in osteosarcoma [21]. However, CPE overexpression can inhibit tumour migration

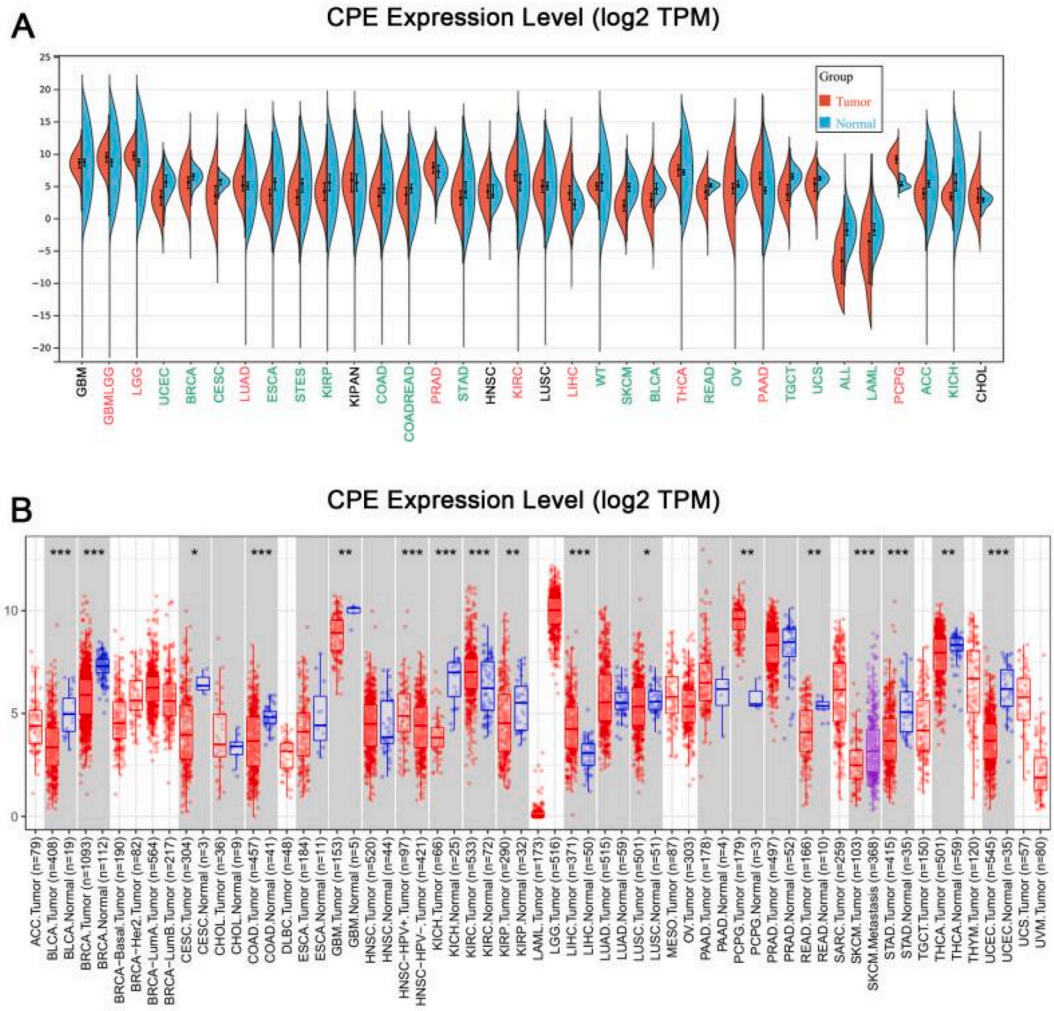

Fig. 1. Pan-cancer analysis revealed transcriptome level variation of CPE in human cancers. (A) Comparison of CPE expression between tumor and normal tissues analysed by SangerBox 3.0. The red−highlighted cancer names indicate that CPE expression was significantly ($p < 0.05$) higher compared to normal tissues. The green−highlighted cancer names indicate that CPE expression was significantly ($p < 0.05$) lower compared to normal tissues. (B) Comparison of CPE expression between tumor and normal tissues analysed by TIMER 2.0. When $P < 0.05$, significant differences were labeled (***$P < 0.001$, **$P < 0.01$, *$P < 0.05$). (TPM: Transcripts Per Million). (For interpretation of the references to colour in this figure legend, the reader is referred to the Web version of this article.)

and improve the prognosis of gliomas [22–24]. Moreover, the functions and mechanisms of CPE in GC are still unclear and require further research.

In the present study, we first explored variations in the transcriptome level and prognostic value of CPE in different types of cancers, and the results indicated that CPE could serve as a prognostic marker for poor survival in GC. Subsequently, we analysed the correlations between clinicopathological characteristics and CPE expression and their potential functions and mechanisms in GC through enrichment analysis using The Cancer Genome Atlas (TCGA) and Gene Expression Omnibus (GEO) databases. In addition, tumour-infiltrating immune cells of CPE were investigated using various methods, and macrophage correlation analysis was conducted. Moreover, this study developed a prognosis prediction nomogram based on CPE, which combined genomic features with clinicopathological characteristics that could improve the accuracy of prognosis prediction at different time points and provide additional evidence for therapeutic treatment planning in GC.

2. Methods and materials

2.1. Public data sources

We verified the transcriptome level variation of CPE in different types of cancers through pan-cancer analysis. Pan-cancer analysis was investigated by SangerBox 3.0 (http://sangerbox.com/) [25] in Fig. 1A and TIMER 2.0 (http://timer.comp-genomics.org/timer/) [26] in Fig. 1B, the data sources of which primarily came from the TCGA database (http://cancergenome.nih.gov) [27]. The significance of differences was assessed using the Wilcoxon test. RNA-sequencing data and associated clinical details were acquired from the TCGA and GEO (https://www.ncbi.nlm.nih.gov/geo/) databases, including GSE84433 (n = 357) and GSE26253 (n = 432). The corresponding abbreviations for the different types of cancers are summarized in Table S1.

2.2. Prognostic analysis of CPE

All patients from the GSE84433(n = 357) and GSE26253(n = 432) databases were categorised into high- and low-expression groups. The cut-off for the high- and low-expression groups was the median value of CPE expression for prognostic analysis. The high-expression group consisted of those who expressed higher than the median value, whereas the low-expression group consisted of those who expressed lower than the median value. To identify independent prognostic factors, Kaplan–Meier and univariate and multivariate Cox regression analyses were performed. Significance was assessed using the log-rank test and hazard ratios (HR) with 95 % confidence intervals (CIs). We further verified the prognostic value of CPE in GC using the Gene Expression Profiling Interactive Analysis (GEPIA) database (http://gepia.cancer-pku.cn/) [28], whose data were acquired from the TCGA database.

2.3. Association between CPE and clinicopathological characteristics in GC

The expression profiles of CPE were retrieved from the TCGA (n = 372) and GSE84433 (n = 357) databases, and the association between CPE and the clinicopathological characteristics of GC patients was visualised in a landscape using R software. The significance of the differences was determined using the Wilcoxon rank-sum test.

2.4. Enrichment analysis

Gene Ontology (GO), Kyoto Encyclopedia of Genes and Genomes (KEGG) functional enrichment analyses, and gene set variation analysis (GSVA) were performed to investigate the biological functions and pathways related to CPE. We selected the top 400 genes significantly correlated (all P-values <0.05) with CPE in descending order based on Pearson's correlation coefficients through analysis in the TCGA and GSE84433 databases. After updating the gene sets to the Database for Annotation, Visualisation, and Integrated Discovery (DAVID) (https://david.ncifcrf.gov/), GO and KEGG analyses were performed. The top six items are displayed in ascending order of P-values.

2.5. Gene set variation analysis

The hallmark gene sets were obtained from the molecular signature database of the Gene Set Enrichment Analysis (https://www.gsea-msigdb.org/gsea/index.jsp). The functional enrichment score of each patient in the TCGA and GSE84433 databases was calculated using the GSVA package (R environment). A heatmap of the enrichment scores was drawn using the heatmap package (R environment). Pearson's correlation analysis was used to determine the correlation between CPE and hallmark gene sets. Items with P-values less than 0.05 are displayed.

2.6. Protein-protein interactions analysis

The network of protein-protein interactions and the probable roles of CPE were predicted and summarized using GeneMANIA (https://www.genemania.org) [29].

2.7. Immune cell infiltration analysis

The ESTIMATE package [30] (R environment) was used to calculate the Immune Score (ratio of immune components), Stromal Score (ratio of stromal components), and estimated score (total of the above two scores). This study extracted the gene expression profiles of GC patients from the TCGA database and carried out a log2 (x+0.001) transformation. Higher scores indicates a larger quantity of the corresponding component in the tumour environment. In addition, the IOBR package [31] (R environment) was used to estimate the abundance of multiple immune cell infiltrations in tumour samples using the EIPC [32], TIMER [26], and Quantiseq [33] algorithms. The relationships between CPE expression and genetic biomarkers of M1 and M2 macrophages, as well as tumour-associated macrophages (TAMs) in GC, were further analysed using TIMER. To assess the significance, the Corr. test was used to calculate Pearson's correlation coefficients between gene expression and immune cell infiltration using the psyche package (R environment).

2.8. Immunohistochemistry and haematoxylin staining

The tissue microarray (including 101 GC tissues and 79 adjacent non-tumour tissues) was obtained from OUTDO Biotech (Shanghai, China). Primary antibody against CPE (human; diluted 1:50) was purchased from Proteintech Group, Inc. (13710-1-AP,

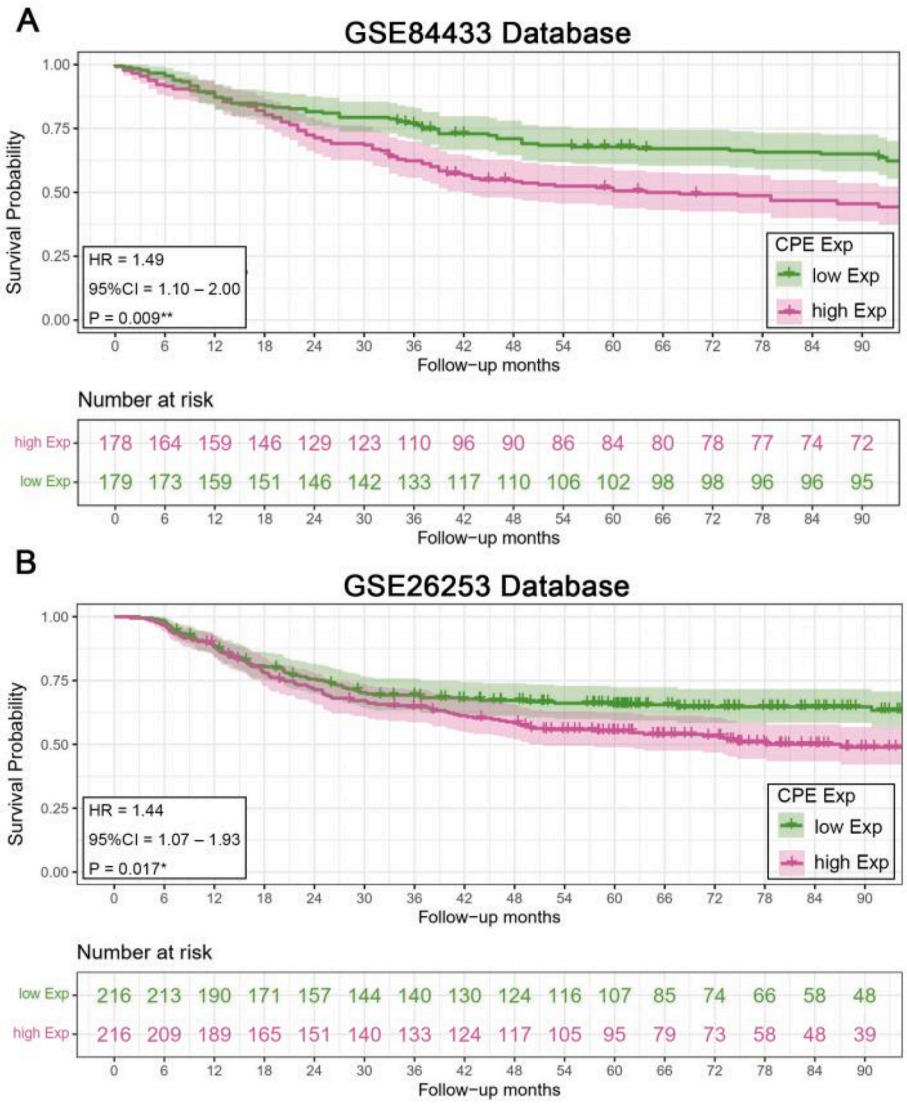

Fig. 2. Kaplan-Meier analysis for CPE. (A) The impact of CPE on overall survival (OS) in GC was investigated using the GSE84433(n = 357) database. (B) The impact of CPE on disease-free survival (DFS) in GC was investigated using the GSE26253(n = 432) database. The log-rank test was used to assess the significance of prognostic value.

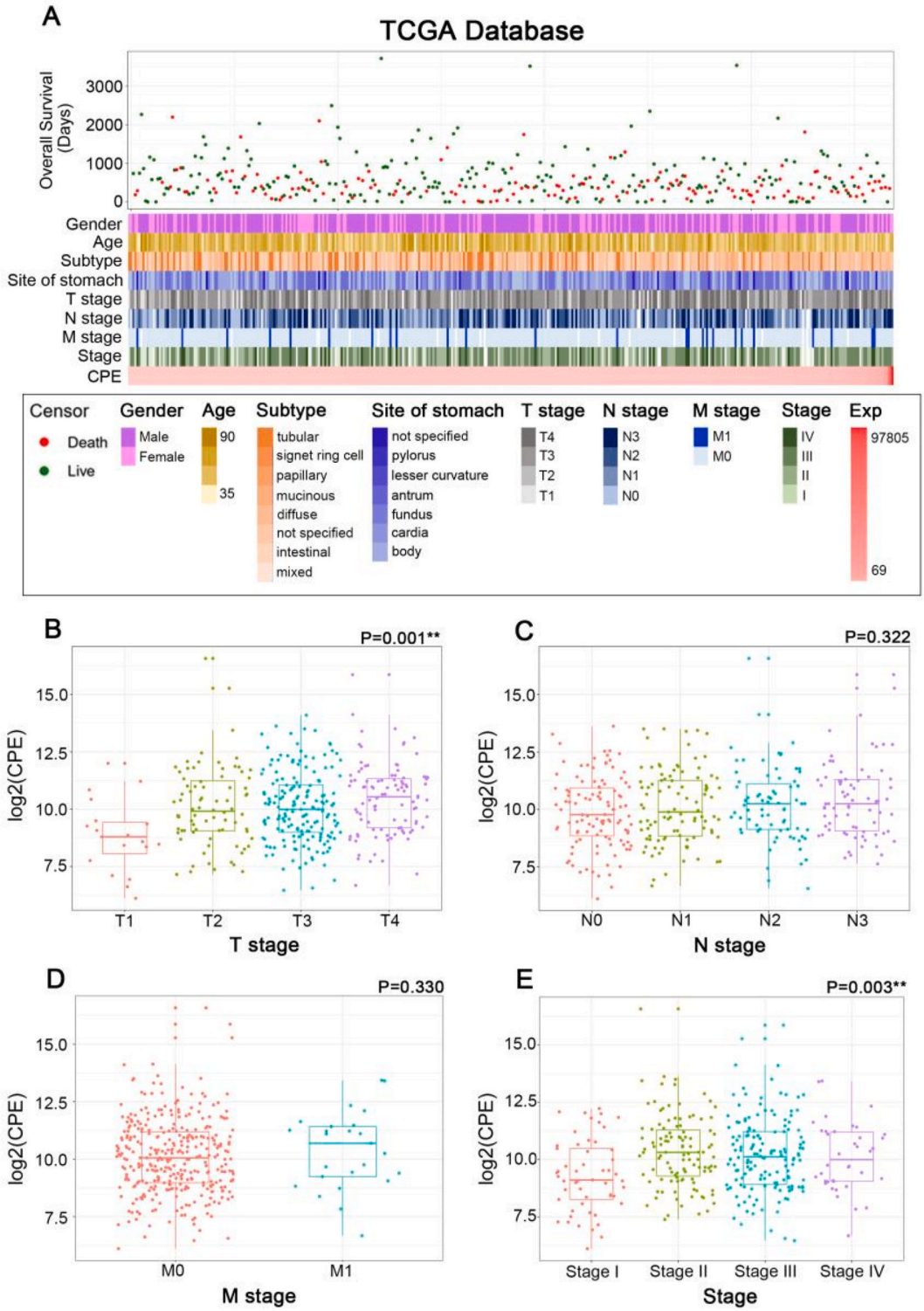

Fig. 3. (A) The correlation between CPE expression and clinicopathological characteristics of GC in the TCGA database was displayed by landscape. CPE expression was substantially increased in higher T stage (B) and GC stage (E) of GC. (C) There was no statistical significance identified between CPE expression and N stage. One-way ANOVA was used to assess the significance of differences mentioned above. (D) There was no statistical significance identified between CPE expression and M stage. The unpaired *t*-test was used to assess the significance of differences.

Wuhan, China). After deparaffinization with xylene, paraffin sections were rehydrated. Tissue sections were filled with EDTA (pH 9.0) for antigen retrieval. After hydrogen peroxide treatment, the sections were incubated at room temperature in the dark for 25 min. The tissues were sealed for 30 min in 3 % BSA at room temperature and incubated for the entire night at 4 °C with the primary antibody against CPE (1:50, 13710-1-AP, Proteintech Group Inc., Wuhan, China). After cleaning, the tissues were incubated with a goat anti-rabbit secondary antibody (1:200, GB23303, Servicebio, China) (HRP-labeled) at room temperature for 50 min. The tissues were initially stained with a diaminobenzidine (DAB) colour developing solution, followed by counterstaining with haematoxylin stain solution, dehydration, and coverslip sealing. The haematoxylin-stained nucleus was blue, whereas the DAB-positive reaction was brownish yellow.

The immunohistochemistry (IHC) scores of CPE proteins were separately assessed by two proficient pathologists according to the IHC staining results. The staining intensity scores were evaluated as 0 (negative staining), 1 (slight staining), 2 (moderate staining), and 3 (strong staining). The percentage of positive cells was scored as 0 (<10 %), 1 (10–25 %), 2 (25–50 %), and 3 (>50 %). The final IHC score was determined by combining the two scores. IHC scores ranging from 3 to 6 indicated high CPE expression, whereas scores between 0 and 2 suggested low CPE expression.

2.9. Establishment and verification of a prognosis predicting model in GC

A nomogram model for prognosis prediction based on CPE was established using the rms package (R environment), with 30 % of GC patients in TCGA as the validation group and 70 % as the training group. The evaluation system is located in the upper region of the nomogram model, whereas the prediction system is located in the lower region. The sum of the individual factor values precisely estimated the 1-, 2-, and 3-year survival probabilities of TCGA group patients. Patients in the validation group were used to examine the prediction precision. Subsequently, calibration curves and C-index values were used to illustrate the accuracy of the prognosis

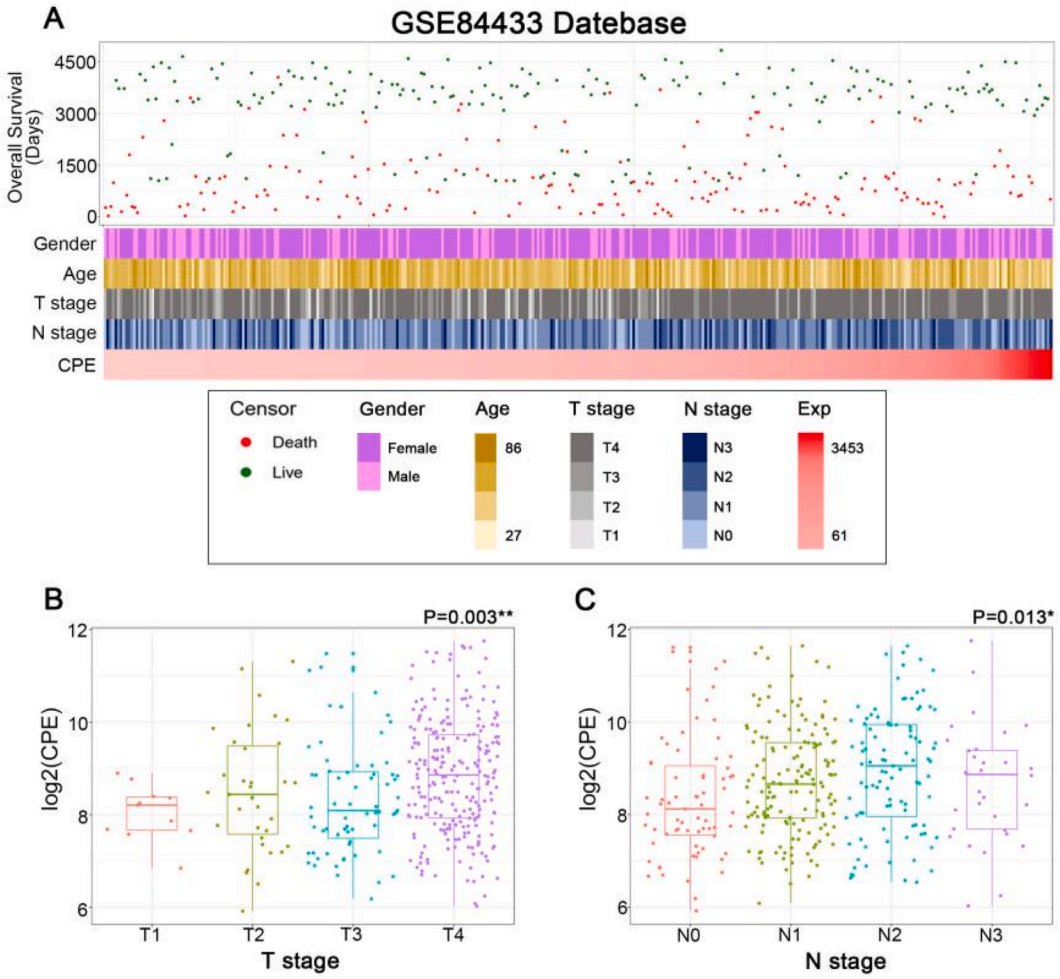

Fig. 4. (A) The correlation between CPE expression and clinicopathological characteristics of GC in the GSE84433 database was displayed by the landscape. CPE expression was substantially increased in higher T (B) and N (C) stages. One-way ANOVA was used to assess the significance of differences mentioned above.

prediction model.

2.10. Statistical analysis

Statistical analyses were performed using R version 4.2.2 and SPSS 20.0. Kaplan–Meier analysis with the log-rank test was performed to evaluate the prognostic value. Univariate and multivariate Cox regression analyses were performed to identify independent prognostic factors.

3. Results

3.1. Transcriptome level variation of CPE in human cancers

CPE expression in different types of cancer and normal control samples was analysed using Sangerbox 3.0 (Fig. 1A) and TIMER 2.0 (Fig. 1B). Compared to that in normal tissues, both methods revealed significantly higher CPE expression in three types of cancers,

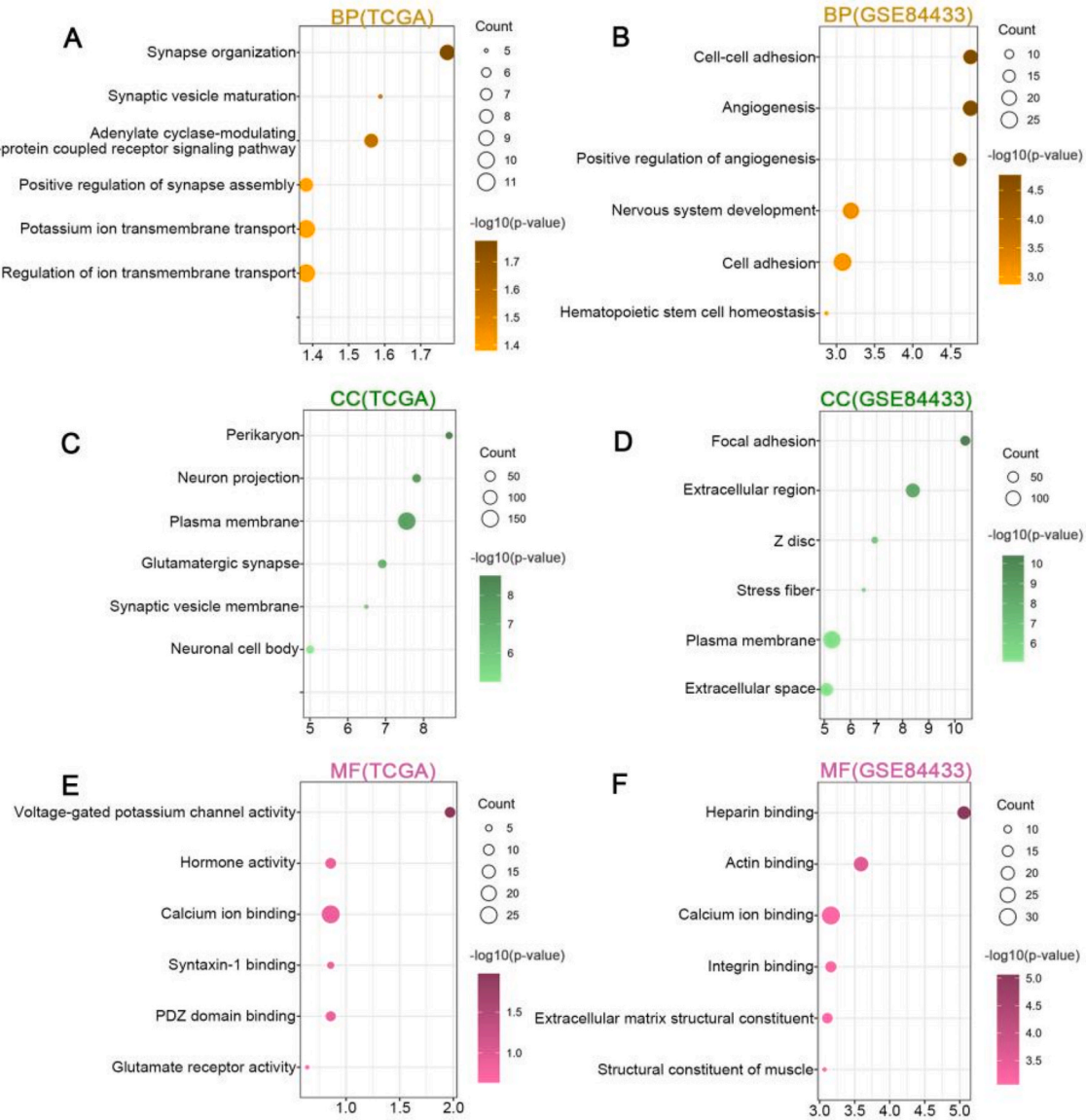

Fig. 5. Functional Enrichment Analysis of CPE. In the TCGA database, the biological processes (A), cellular components (C), and molecular functions (E) most closely related to CPE are shown. In the GSE84433 database, the biological processes (B), cellular components (D), and molecular functions (F) most closely related to CPE are shown.

including kidney renal clear cell carcinoma, liver hepatocellular carcinoma, and pheochromocytoma and paraganglioma. Additionally, both methods revealed that CPE expression was significantly downregulated in eight types of cancers, including bladder urothelial carcinoma, breast invasive carcinoma, cervical squamous cell carcinoma and endocervical adenocarcinoma, colon adenocarcinoma, kidney chromophobe, kidney renal papillary cell carcinoma, rectum adenocarcinoma, and stomach adenocarcinoma.

3.2. Prognostic value of CPE

The impact of CPE on disease-free survival (DFS) and overall survival (OS) in GC was investigated using the GSE84433(n = 357) and GSE26253(n = 432) databases and GEPIA. Patients in the GSE84433 and GSE26253 databases were categorised into high- and low-expression groups based on the median value of CPE expression. Analysis of the prognostic value revealed that poorer OS (Fig. 2A and Fig. S1A) and DFS (Fig. 2B and Fig. S1B) were associated with increased CPE expression in gastric tumour tissue. Elevated CPE expression was associated with poor OS in GC patients in GEPIA (HR = 1.40, P = 0.049) and GSE84433 (HR = 1.49, P = 0.009), as well as unfavourable DFS in GEPIA (HR = 1.50, P = 0.033) and GSE26253 (HR = 1.44, P = 0.017).

Additionally, in patients with different types of cancer, the effect of CPE on (OS was analysed via Sangerbox 3.0 (Fig. S2). Patients with higher CPE expression had poor OS in seven types of cancers, including TCGA-CESC (N = 273, P = 6.5e-3, HR = 1.17), TCGA-STES (N = 547, P = 0.01, HR = 1.10), TCGA-KIPAN (N = 855, P = 4.7e-3, HR = 1.10), TCGA-PRAD (N = 492, P = 0.02, HR = 2.17), TCGA-STAD (N = 372, P = 5.1e-4, HR = 1.18), TCGA-BLCA (N = 398, P = 1.3e-3, HR = 1.16), and TARGET-ALL (N = 53, P = 0.04, HR = 1.29). Patients with lower CPE expression had poor OS in four types of cancers, including TCGA-GBMLGG (N = 619, P = 1.8e-20, HR

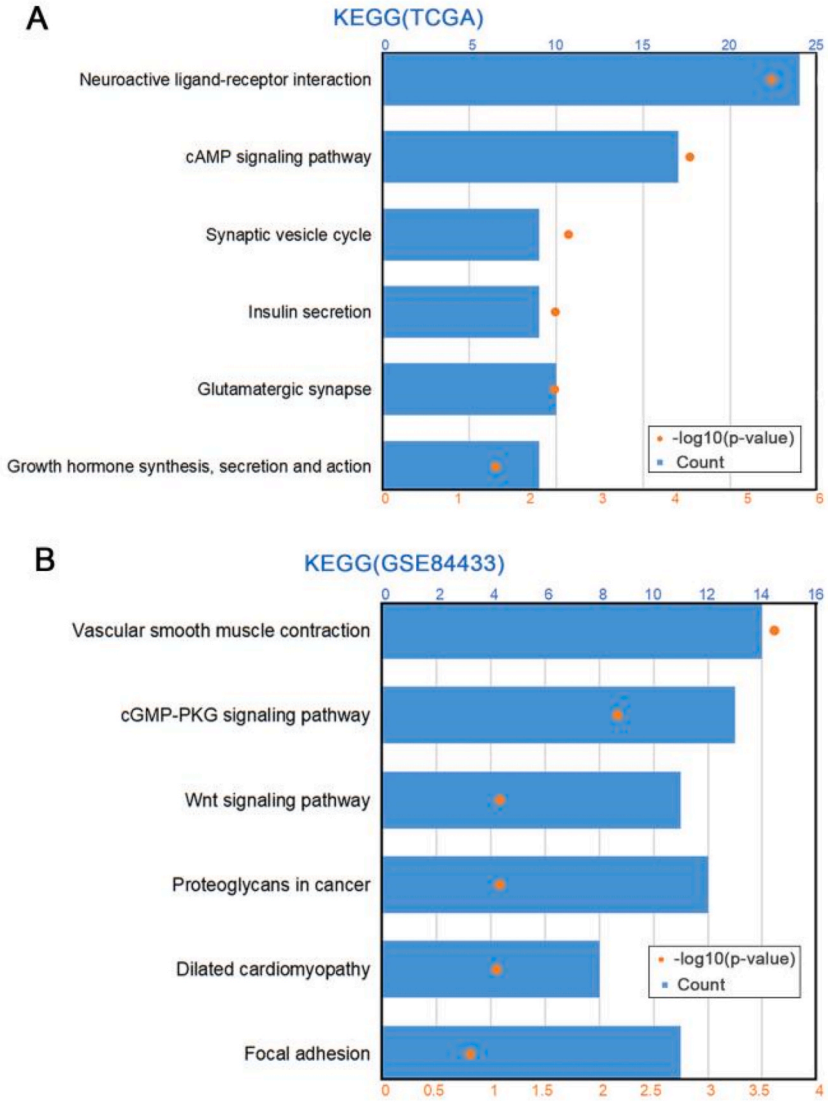

Fig. 6. Kyoto Encyclopedia of Genes and Genomes (KEGG) pathway analysis of CPE in the databases TCGA (A) and GSE84433 (B).

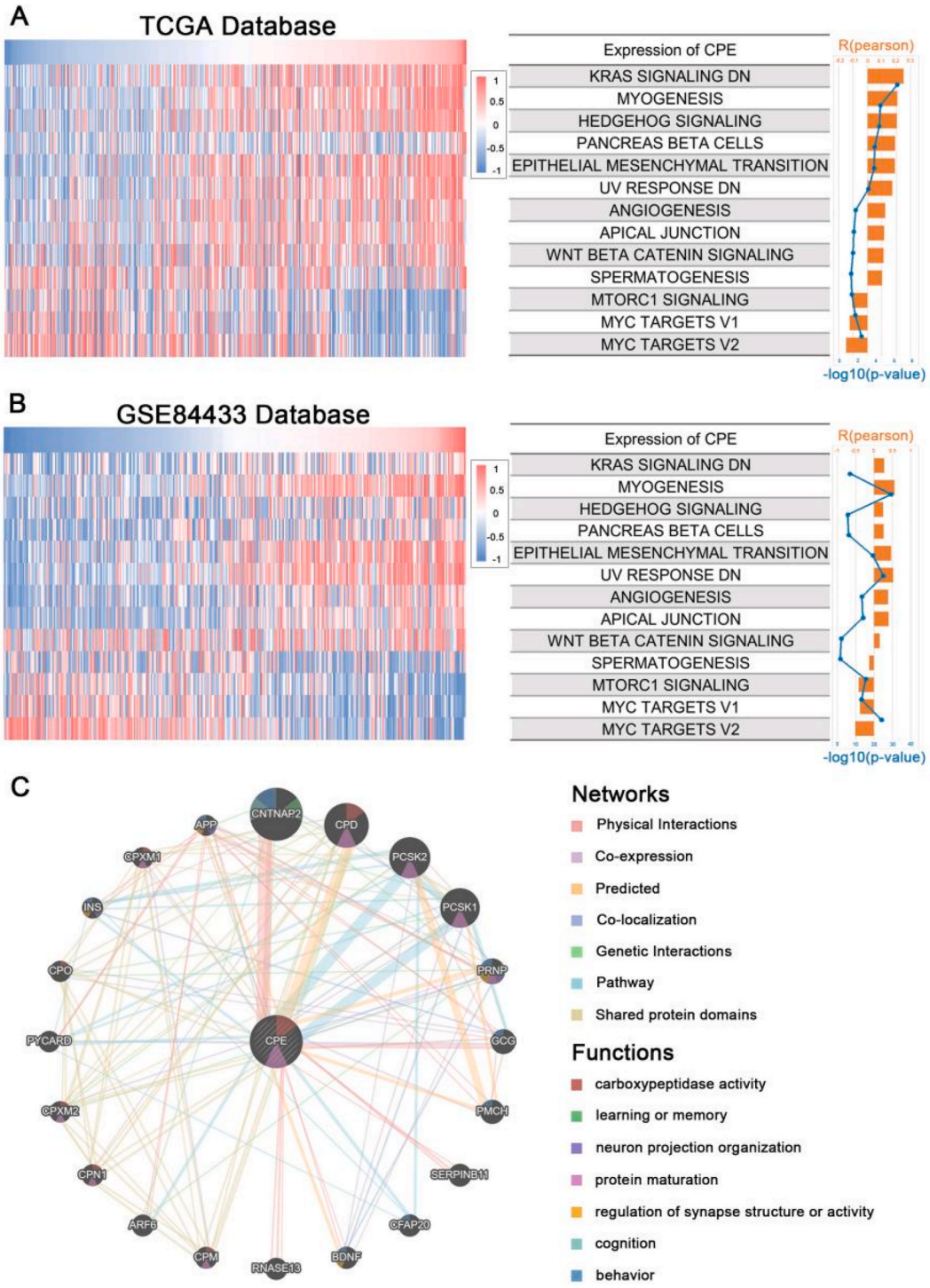

Fig. 7. Gene set variation analysis (GSVA) between CPE expression and hallmark gene sets enrichment scores. The heatmap displays the relationship between CPE expression and the enrichment scores of hallmark gene sets of each patient from the TCGA (A) and GSE84433 (B) databases. The R-value and P-value of the correlation analysis are displayed in the column and line graphs on the right respectively. (C) The protein-protein interaction (PPI) network and potential functions of CPE were analysed by the GeneMANIA tool.

= 0.62), TCGA-LGG (N = 474, P = 5.4e-6, HR = 0.67), TARGET-NB (N = 151, P = 5.1e-5, HR = 0.54), and TCGA-PAAD (N = 172, P = 0.02, HR = 0.87).

3.3. CPE and clinicopathological characteristics in GC patients

Various clinicopathological characteristics were observed in patients with different CPE expression levels. Landscapes representing the vital status of all patients in the TCGA (Fig. 3A) and GSE84433 (Fig. 4A) databases at various time points were created, and the corresponding clinicopathological information is presented in bar charts in different colours. CPE expression was substantially increased at higher T stage (P = 0.001) (Fig. 3B) and GC stage (P = 0.003) (Fig. 3E). In the GSE84433 database, CPE expression followed the same pattern. CPE expression was significantly correlated with T (P = 0.003) and N stages (P = 0.013) (Fig. 4B and C). No statistically significant association was observed between CPE expression and other clinicopathological characteristics, including N (Fig. 3C) and M stages (Fig. 3D). In summary, evidence indicates that CPE expression increased in GC at later stages of the disease.

3.4. GSVA and Functional Enrichment Analysis of CPE

In the TCGA database, the biological processes that correlated the most with CPE consisted of *synapse organization* and *synaptic vesicle maturation* (Fig. 5A). Furthermore, *perikaryon* and *plasma membrane* were two of the most closely related cellular components of

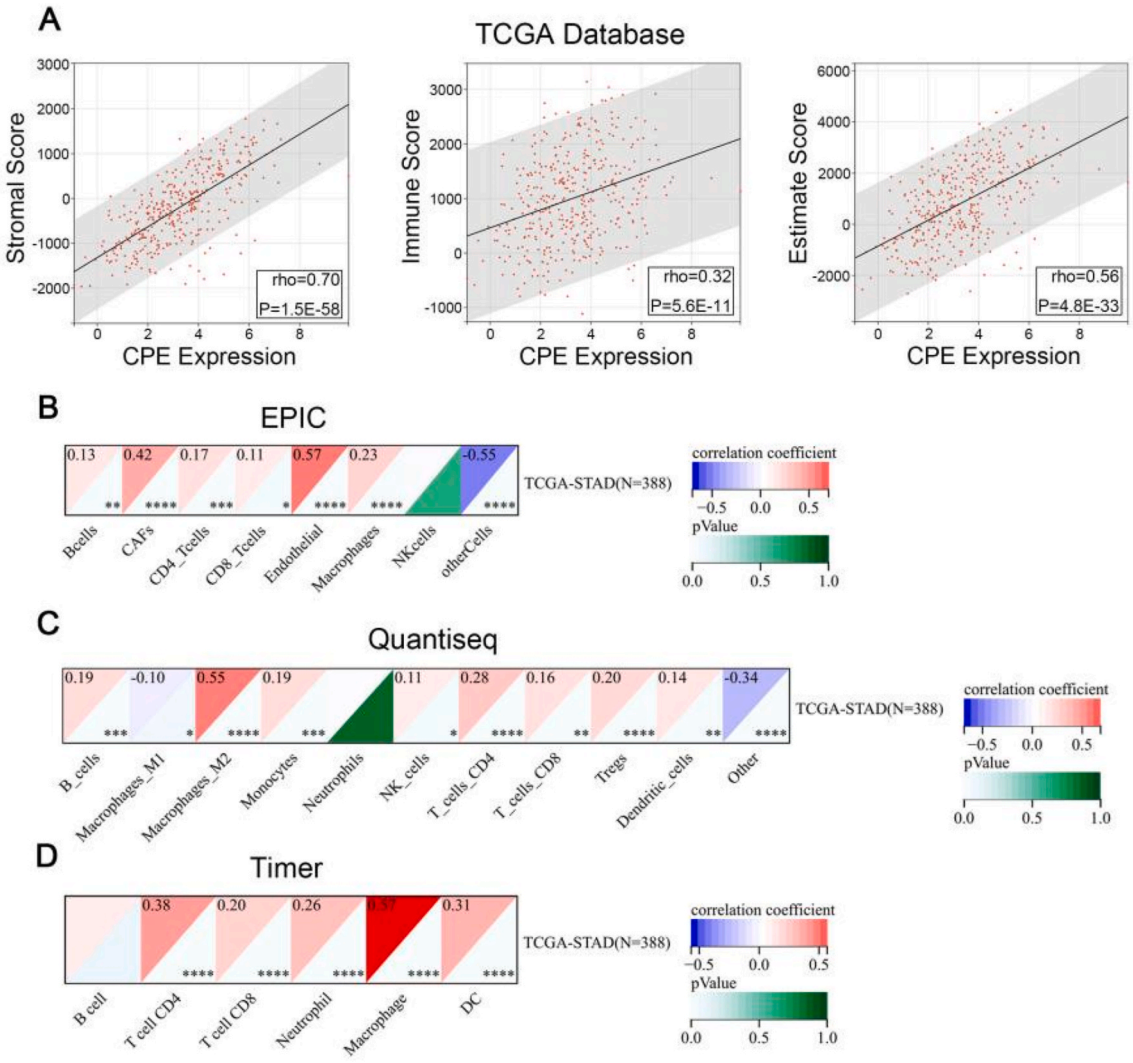

Fig. 8. The correlation between CPE expression and immune cell infiltration in GC. (A) Stromal, Immune, and Estimate Scores were calculated and presented by scatter plots. The EIPC (B), Quantiseq (C), and Timer (D) algorithms were used to analyse GC samples from the TCGA database to assess the level of immune cell infiltration. Pearson's correlation coefficients between CPE expression and immune cell infiltration scores in GC were calculated. When P < 0.05, significant differences were labeled (***P < 0.001, **P < 0.01, *P < 0.05).

CPE (Fig. 5C). *Hormone activity* and *voltage-gated potassium channel activity* were examples of molecular functions of CPE (Fig. 5E). The two signalling pathways most closely related to CPE were *neuroactive ligand-receptor interaction* and *cAMP signalling pathway* (Fig. 6A). The biological processes, cellular components, molecular functions, and signalling pathways correlated with CPE in the TCGA database were subsequently verified using the GSE84433 database (Fig. 5B, D, F and 6B).

In the GSE84433 database, *Cell-cell adhesion* and *angiogenesis* were biological processes that exhibited a strong correlation with CPE. (Fig. 5B). Moreover, *focal adhesion* and *extracellular region* were two of the most closely related cellular components of the CPE (Fig. 5D). *Integrin binding* and *extracellular matrix structural constituent* were examples of the molecular functions of CPE (Fig. 5F). *Wnt signalling pathway* and *cGMP-PKG signalling pathway* were the most closely related to CPE (Fig. 6B).

GSVA between the enrichment score of the hallmark gene sets and CPE expression revealed a positive correlation with *Hedgehog signalling*, *angiogenesis*, *epithelial-mesenchymal transition*, and *Wnt β-catenin signalling* and a negative correlation with *mTORC1 signalling*

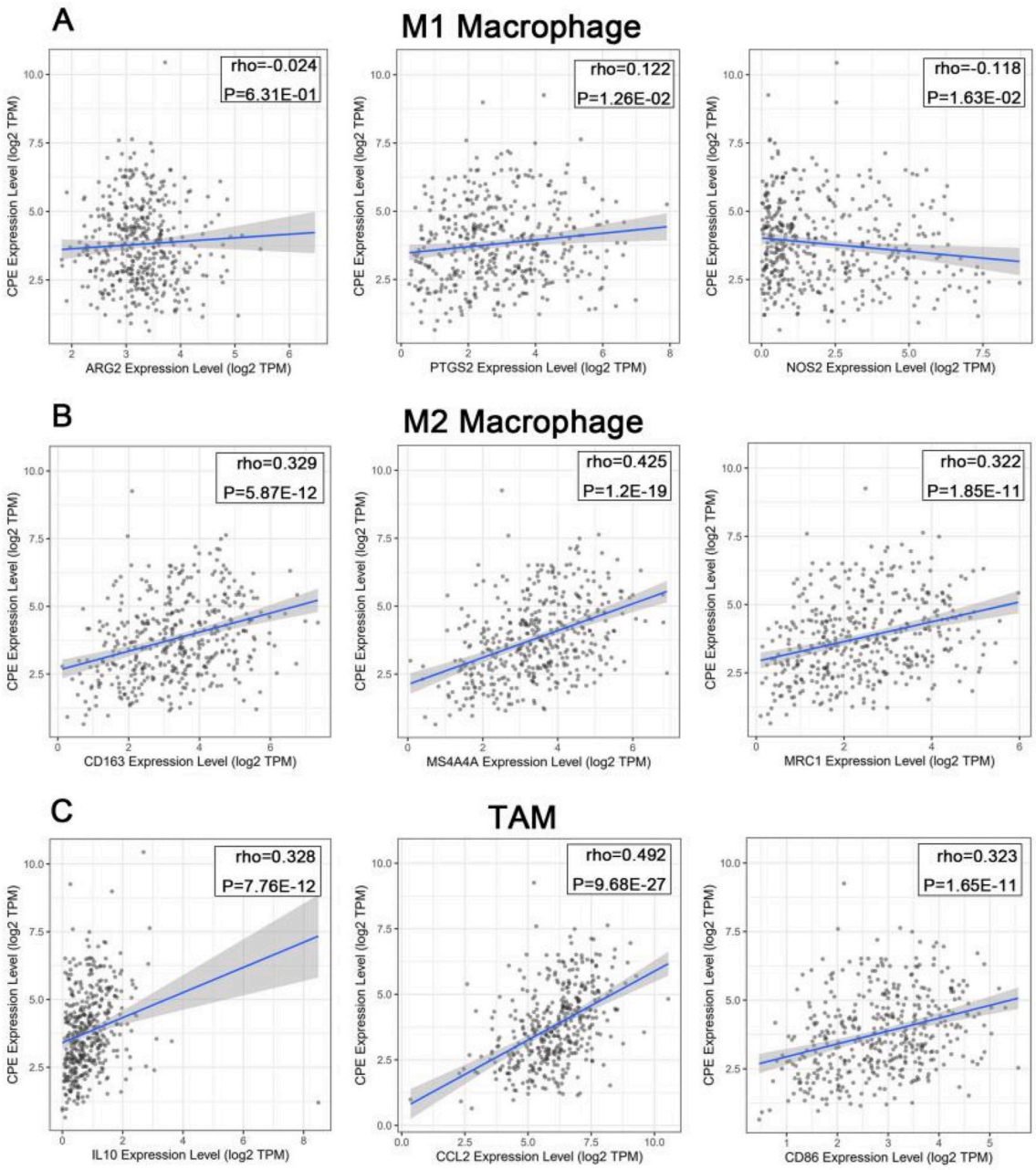

Fig. 9. Correlation between CPE expression and macrophage polarisation in GC. The correlations between CPE expression and genetic biomarkers of M1 macrophages (ARG2, PTGS2, and NOS2) (A), M2 macrophages (CD163, MS4A4A, and MRC1) (B), and TAMs (IL10, CCL2, and CD86) (C) are displayed in scatterplot form.

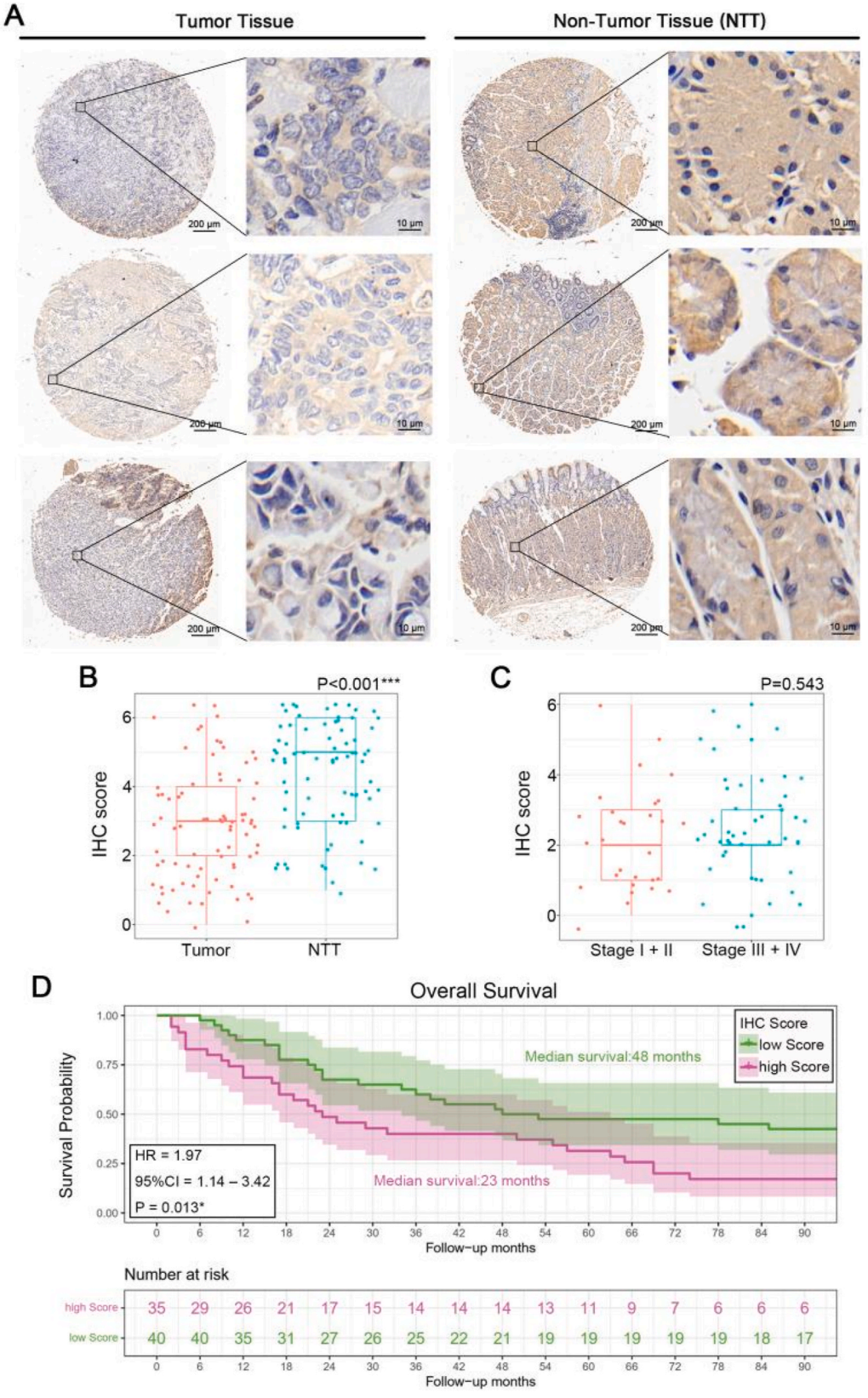

(caption on next page)

Fig. 10. Overexpression of CPE indicated poor clinical prognosis in GC. (A) Representative CPE Immunohistochemistry staining of tissue microarray. (B) Tumor tissues had significantly lower levels of CPE protein expression than non-tumor tissues (NTTs). (C) There was no statistical significance identified between CPE protein expression and Stage. (D) Relationship Between CPE and Poor Prognosis Revealed by Immunohistochemistry Analysis of tissue microarray.

in the TCGA database (Fig. 7A). These findings were further confirmed using the GSE84433 database (Fig. 7B). CPE appears to play an important role in GC tumourigenesis by mediating tumour cell proliferation and metastasis.

Using the GeneMANIA tool, we generated a protein-protein interaction network to investigate the potential functions of the CPE in more detail. Twenty genes were found to interact with CPE (Fig. 7C). This suggests that CPE was associated with *learning or memory*, *protein maturation*, *neuron projection organization*, *carboxypeptidase activity*, *regulation of synapse structure or activity*, *cognition* and *behaviour*.

3.5. Estimation for stromal, immune, and Estimate Scores

Higher percentages of immunological or stromal elements were reflected in higher immunological or stromal scores. The estimated score represented tumour purity and was determined by the sum of the immune and stromal scores.

The findings suggest that the three scores were positively correlated with CPE expression and increased significantly as CPE expression progressed (all P-values <0.05) (Fig. 8A). CPE expression significantly impacted the immune response in GC environment.

Table 1
In the TCGA database, overall survival of GC was analysed using univariate and multivariate Cox regression analyses to identify independent prognostic factors. P-value <0.05 was considered statistically significant.

Univariate and multivariate analysis of prognostic parameters in TCGA database overall survival (OS)				
Characteristics	**Univariate analysis**		**Multivariate analysis**	
	Hazard ratio (95 % CI)	**P value**	**Hazard ratio (95 % CI)**	**P value**
CPE expression	1.154(1.044–1.276)	**<0.01**	1.190(1.058–1.339)	**<0.01**
Age	1.025(1.008–1.042)	**<0.01**	1.039(1.018–1.060)	**<0.001**
Gender				
Female	Reference			
Male	1.279(0.899–1.819)	0.171		
Subtype				
Tubular	Reference			
Signet ring cell	2.217(0.999–4.919)	0.050	2.164(0.845–5.546)	0.108
Papillary	1.765(0.533–5.852)	0.353	3.663(1.038–12.926)	**<0.05**
Mucinous	0.299(0.090–0.991)	**<0.05**	0.366(0.107–1.251)	0.109
Diffuse	1.037(0.590–1.823)	0.899	1.397(0.740–2.637)	0.302
Intestinal	1.290(0.768–2.165)	0.336	1.644(0.944–2.862)	0.079
Mixed	0(0–1.067E+170)	0.961	0(0–6.749E+195)	0.964
Site of stomach				
Body	Reference			
Cardia	1.164(0.737–1.839)	0.514		
Fundus	0.982(0.528–1.825)	0.954		
Antrum	1.076(0.701–1.651)	0.738		
Lesser curvature	0(0–9.466E+124)	0.948		
Pylorus	1.108(0.463–2.650)	0.818		
T stage				
T1	Reference			
T2	6.013(0.816–44.281)	0.078	3.197(0.399–25.589	0.274
T3	8.667(1.204–62.408)	**<0.05**	4.597(0.517–40.884)	0.171
T4	8.582(1.178–62.509)	**<0.05**	3.948(0.432–36.050)	0.224
N stage				
N0	Reference			
N1	1.586(0.980–2.566)	0.060	1.317(0.646–2.684)	0.449
N2	1.582(0.941–2.661)	0.084	1.259(0.520–3.051)	0.610
N3	2.588(1.603–4.179)	**<0.001**	1.831(0.756–4.434)	0.180
M stage				
M0	Reference			
M1	2.218(1.275–3.861)	**<0.01**	0.997(0.411–2.415)	0.994
Stage				
Stage I	Reference			
Stage II	1.531(0.774–3.031)	0.221	0.954(0.336–2.705)	0.929
Stage III	2.285(1.205–4.332)	**<0.05**	1.139(0.284–4.559)	0.854
Stage IV	3.830(1.866–7.863)	**<0.001**	2.468(0.579–10.514)	0.222

3.6. Correlation between CPE expression and immune cell infiltration

EPIC algorithm revealed CPE's strong correlation with immune cell infiltration in GC, including B cells (R = 0.13), cancer-associated fibroblasts (R = 0.42), CD4+T cells (R = 0.17), CD8+T cells (R = 0.11), the endothelium (R = 0.57), and macrophages (R = 0.23) (Fig. 8B). As shown in Fig. 8C, Quantiseq algorithm was used to find whether CPE was significantly correlated with the infiltration levels of B cells (R = 0.19), M1 macrophages (R = −0.10), M2 macrophages (R = 0.55), monocytes (R = 0.19), NK cells (R = 0.11), CD4+T cells (R = 0.28), CD8+T cells (R = 0.16), Tregs (R = 0.20), and dendritic cells (R = 0.14). By applying the TIMER algorithm, we found that CPE was strongly correlated with the infiltration levels of neutrophils (R = 0.26), dendritic cells (R = 0.31), CD4+T cells (R = 0.38), CD8+T cells (R = 0.20), macrophages (R = 0.57), and neutrophils (R = 0.26) (Fig. 8D). Summarily, CPE significantly correlated with immune cell infiltration in GC.

3.7. Relationship between CPE expression and macrophages

Quantiseq analysis revealed that the number of M1 macrophages dramatically downregulated in the group with high CPE expression, whereas that of M2 macrophages was significantly upregulated (Fig. 8C), suggesting that CPE had an impact on M2 macrophage polarisation. We further investigated the relationship between CPE expression and genetic biomarkers of different macrophage subtypes, including M1 and M2 macrophages, as well as TAMs in GC using TIMER. The correlation between CPE expression and genetic biomarkers of M1 macrophages, such as PTGS2 (R = 0.12) and NOS2 (R = −0.12), was weak (Fig. 9A). In contrast, the results indicate that the genetic biomarkers of M2 macrophages, such as CD163 (R = 0.33), MRC1 (R = 0.32), and MS4A4A (R = 0.43), were strongly correlated (Fig. 9B). Genetic biomarkers of TAMs such as CD86 (R = 0.32), CCL2 (R = 0.49), and IL10 (R = 0.33) were also strongly correlated (Fig. 9C). Overall, our findings suggest that elevated CPE levels played a regulatory role in the polarisation of M2 macrophages and their differentiation into TAMs.

3.8. Relationship between CPE and Poor Prognosis Revealed by Immunohistochemistry Analysis of tissue microarray

A tissue microarray comprising 101 GC tissues and 79 adjacent non-tumour tissues (NTT) was acquired from OUTDO Biotech (Shanghai, China) and used in our investigation (Fig. 10A). In our investigation, NTT cells showed substantially higher levels of CPE protein expression than those of tumour tissues (Fig. 10B). However, there was no discernible correlation between Stage and CPE protein expression (Fig. 10C). Additionally, overexpression of CPE indicated poor OS in GC (HR = 1.97, 95 % CI = 1.14–3.42, p = 0.013), as shown in Fig. 10D, where patients with higher CPE expression had significantly shorter OS (median survival: 23 months) compared to those with lower CPE expression (median survival: 48 months).

3.9. CPE as an independent prognostic factor in GC

Univariate and multivariate Cox regression analyses demonstrated that CPE expression was an independent predictor, regardless of other clinicopathologic factors, such as age, sex, subtype, stomach site, T stage, M stage, N stage, and Stage in the TCGA database (Table 1) and age, sex, T stage, and N stage in the GSE84433 database (Table 2). These results indicate that CPE acted as an independent prognostic factor in GC.

Table 2
In the GSE84433 database, overall survival of GC was analysed using univariate and multivariate Cox regression analyses to identify independent prognostic factors. P-value <0.05 was considered statistically significant.

Univariate and multivariate analysis of prognostic parameters in GSE84433 database overall survival (OS)				
Characteristics	**Univariate analysis**		**Multivariate analysis**	
	Hazard ratio (95 % CI)	**P value**	**Hazard ratio (95 % CI)**	**P value**
CPE expression	1.196(1.066–1.343)	**<0.01**	1.174(1.041–1.324)	**<0.01**
Age	1.019(1.005–1.033)	**<0.01**	1.021(1.007–1.035)	**<0.01**
Gender				
Female	Reference			
Male	1.266(0.910–1.762)	0.161		
T stage				
T1	Reference			
T2	1.023(0.212–4.926)	0.977		
T3	2.489(0.593–10.452)	0.213		
T4	3.942(0.976–15.928)	0.054		
N stage				
N0	Reference			
N1	1.606(0.991–2.603)	0.054	1.556(0.958–2.528)	0.074
N2	3.245(1.996–5.276)	**<0.001**	2.960(1.806–4.851)	**<0.001**
N3	4.132(2.279–7.492)	**<0.001**	3.957(2.180–7.181)	**<0.001**

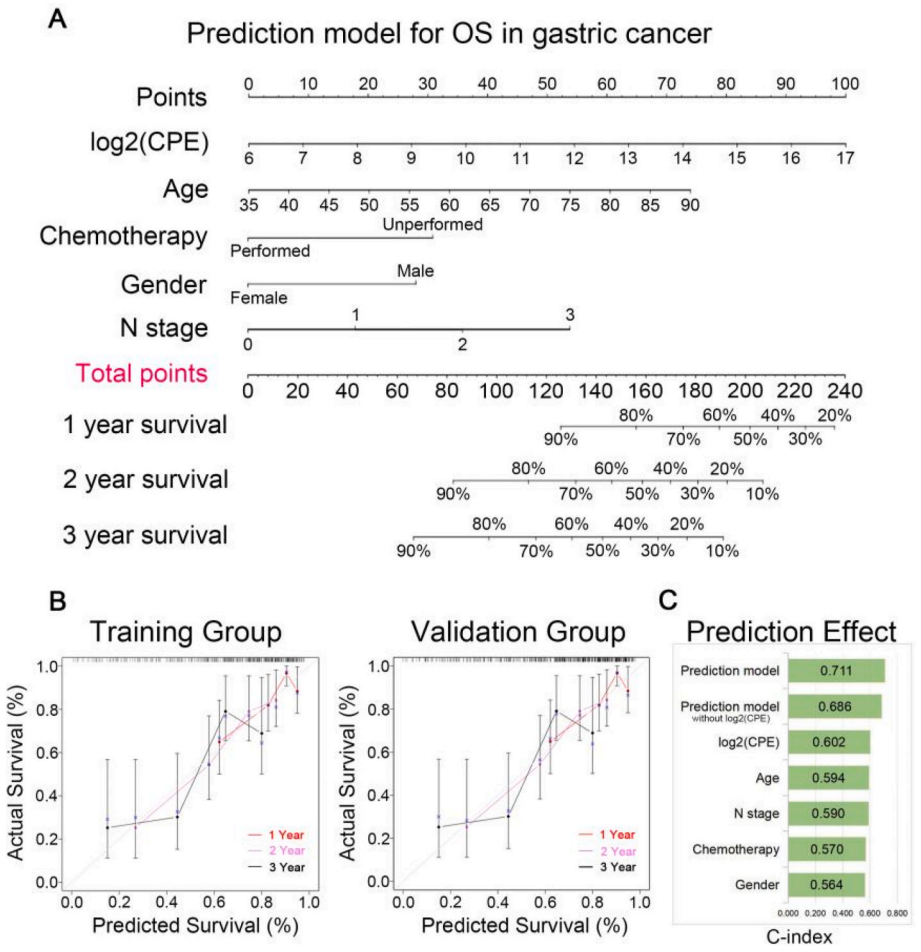

Fig. 11. The nomogram model for prognosis prediction of OS in GC. (A) The nomogram model could precisely predict the 1-, 2-, and 3-year survival probabilities of patients with GC. (B) Calibration curves showed the comparison between predicted and actual OS for 1-, 2-, and 3-year survival probabilities in training and validation groups. (C) The predictive effect on survival probability of individualised prediction model, prediction model without CPE expression, CPE expression, and other clinical prognostic characteristics of GC was assessed by C-Index.

3.10. Construction of clinical individualised prognosis prediction model

Using the rms package (R environment), predictive parameters with the best predictive effects were selected to construct a customised prediction model for OS prediction. CPE expression, age, sex, N stage, and chemotherapy status were included among the variables. As shown in Fig. 11A, the individualised prediction nomogram model estimated the 1-, 2-, and 3-year OS probabilities in GC. The nomogram and actual observations in the calibration curves showed sufficient overlap in the training and validation groups, indicating a desirable prediction accuracy (Fig. 11B). This nomogram model had a C-index of 0.711, which was higher than that of the other prediction models (Fig. 11C).

4. Discussion

Certain biomarkers may be associated with tumourigenesis, cancer development, and survival in patients diagnosed with cancer [34,35]. According to previous research, although CPE could influence the proliferation and metastasis of tumour cells in various types of cancers and is associated with tumourigenesis [11,17,19,21,36–38], its prognostic value and molecular mechanism in GC remain unclear. Based on our findings, CPE may act as an oncogene and promote GC development.

CPE expression in different types of cancer and normal control samples was analysed using Sangerbox 3.0 (Fig. 1A) and TIMER 2.0 (Fig. 1B), which suggested that CPE expression is downregulated in GC compared to normal tissue. The results of Kaplan-Meier analysis of the TCGA and GSE84433 databases suggested that poorer OS (Fig. 2A) and DFS (Fig. 2B) were associated with increased CPE expression in gastric tumour tissue. Furthermore, CPE was considered to be an independent prognostic factor in GC verified by univariate and multivariate Cox regression analyses. Using these bioinformatics analyses, we found that CPE overexpression may contribute to a poor prognosis in GC. We verified the prognostic value of CPE via immunohistochemistry and haematoxylin staining of

tissue microarray, and found that, overexpression of CPE indicated poor OS in GC (HR = 1.97, 95 % CI = 1.14–3.42, p = 0.013) (Fig. 10D). To investigate the potential functions and mechanisms of CPE in GC, we conducted enrichment analysis on publicly accessible databases. In the GSE84433 database, *focal adhesion* was the most closely related cellular components of the CPE (Fig. 5D). Moreover, *cell-cell adhesion* and *angiogenesis* were biological processes that exhibited a strong correlation with CPE. (Fig. 5B). As shown in Fig. 6B, *Wnt signalling pathway* and *focal adhesion* were the most closely related to CPE according to KEGG analysis. GSVA between the enrichment score of the hallmark gene sets and CPE expression revealed a positive correlation with *angiogenesis*, *epithelial-mesenchymal transition*, and *Wnt β-catenin signalling* in the TCGA database (Fig. 7A). These findings were further confirmed using the GSE84433 database (Fig. 7B).

CPE is present in the extracellular space, bound to a receptor called HTR1E, and activates oncogenic signalling pathways including NF-κB, Wnt3a, and ERK1/2 to control tumour development and metastasis by triggering the expression of target genes involved in anti-apoptotic and cell cycle regulation [39]. Furthermore, CPE increases the production of the anti-apoptotic protein BCL-2 by activating ERK1/2 pathway, which in turn upregulates the expression of the Wnt pathway gene active β-catenin, mediating the survival of hepatocellular carcinoma cells during metabolic stress consequently [18]. Bioinformatics analysis revealed that the p53 signalling pathway, ECM-receptor interaction, focal adhesion, and Wnt signalling pathway were CPE-regulated mechanisms for proliferation in pancreatic tumour cells and are associated with the initiation or development of cancer [40]. In addition, EMT facilitates GC proliferation and migration [41–43] and is crucial for tumour invasion and metastasis [44]. Combining findings of previous studies and the results of our analysis, we hypothesise that CPE overexpression induces EMT through the Erk/Wnt pathway, which promotes proliferation, invasion, and metastasis in GC.

By analyzing the tumour immune microenvironment, we found that CPE expression might impact the immune response and correlate with macrophage infiltration in GC environment. To verify the relationship between CPE expression and macrophages, the TIMER algorithm was further utilized to analyse the association between CPE expression and genetic biomarkers of different macrophage subtypes, including M1 and M2 macrophages, as well as TAMs in GC. The results suggested that there was a weak correlation between CPE expression and genetic biomarkers of M1 macrophages, but a strong correlation was observed between the genetic biomarkers of M2 macrophages and TAM. Elevated CPE levels may play a regulatory role in the polarisation of M2 macrophages and their differentiation into TAMs.

In previous research, tumour-infiltrating immune cells can interfere with tumour progression and are correlated with GC [45]. Macrophages play crucial roles in the digestion and elimination of tumour cells. They differentiate into two main subsets: M1 (classically activated macrophages) and M2 (alternatively activated macrophages). TAMs consist of M2 and some M1 cells, which not only lack the ability to digest tumour cells but also facilitate their migration and metastasis [46]. EMT activated by the Erk/Wnt pathway could be influenced by the high infiltration of TAMs, which is linked to poor prognosis in GC [47]. The effects of TAMs on tumour cell proliferation [48], angiogenesis [49], invasion [50], and metastasis [51] have been documented. Combining findings of previous studies and the results of our analysis, we hypothesise that CPE may promote macrophage polarisation to M2 macrophages and their differentiation into TAMs, which may accelerate EMT, leading to the migration and metastasis of tumour cells; this could ultimately result in a poor prognosis.

However, our study had certain limitations. To validate the role of CPE in GC, the human tissue microarray (including 101 GC tissues and 79 adjacent non-tumour tissues) was evaluated for CPE protein expression via IHC analysis (Fig. 10). However, the limited sample size is a limitation for our current research. More clinical samples should be included to draw a solid conclusion. A larger cohort with multicenter GC patients should be enrolled in the future to further validate the results. Although pre-clinical results suggest CPE as a potential prognostic indicator for GC patients, CPE is not a frequently detected biomarker in clinical practice for cancer, and translational research is warranted. As the results of our bioinformatics analyses were insufficient, additional validation through clinical sample analysis and in vitro and in vivo studies is required. Although CPE expression has been recently reported to play an important role in tumourigenesis and tumour progression, its underlying molecular regulation and detailed biological mechanism should be further validated in the future. We will present more experiments to support the hypothesis and further study the underlying molecular mechanisms of CPE in our future work.

Furthermore, we developed a prognostic nomogram model based on CPE with considerable predictive accuracy for GC. Our nomogram is simple to use and has the potential to be a rapid and effective tool for the individualised prediction of prognosis in GC patients. However, this model had several limitations. Owing to the limited sample size and factors, more clinical samples and characteristics should be included to build a more precise model. As customised prediction models are used more frequently, it is necessary to adjust the model's parameters and predictive elements to increase prediction accuracy.

5. conclusion

Our study revealed the prognostic value and potential mechanisms of CPE in GC. CPE may accelerate GC development through various mechanisms, including the activation of EMT via Erk/Wnt pathways and polarisation of M2 macrophages and their differentiation into TAMs. These insights suggest that CPE could serve as a promising therapeutic target in GC treatment. Moreover, we developed a prognostic nomogram model with considerable prediction accuracy based on CPE.

Funding

This work was supported by Leading Innovation Specialist Support Program of Guangdong Province, the Science and Technology Planning Project of Ganzhou (No. 202101074816), National Key Clinical Specialty Construction Project (2021–2024, No.

2022YW030009), Science and Technology Plan of Guangzhou, Guangdong Province, China (No. 202201011416) and National Natural Science Foundation of China (No.82260501).

Availability of data

The datasets generated and analysed in this study are available in the TCGA (http://cancergenome.nih.gov) and GEO (https://www.ncbi.nlm.nih.gov/geo/) databases. The corresponding author can provide other data upon reasonable requests.

Declarations

No additional ethical approval or informed consent was required as all data were publicly available.

CRediT authorship contribution statement

Jiarui Lin: Writing – original draft, Visualization, Validation, Software, Resources, Methodology, Investigation, Data curation. **Chengzhi Huang:** Validation, Resources, Methodology, Investigation, Conceptualization. **Wenfei Diao:** Software, Resources. **Haoming Liu:** Methodology, Investigation. **Hesong Lu:** Resources, Investigation. **Shengchao Huang:** Software, Resources. **Junjiang Wang:** Supervision, Project administration, Funding acquisition, Formal analysis.

Declaration of competing interest

The authors declare that they have no known competing financial interests or personal relationships that could have appeared to influence the work reported in this paper.

Appendix A. Supplementary data

Supplementary data to this article can be found online at https://doi.org/10.1016/j.heliyon.2024.e29901.

References

[1] Global Cancer Statistics, GLOBOCAN Estimates of Incidence and Mortality Worldwide for 36 Cancers in 185 Countries, 2020.
[2] D. Sidransky, Emerging molecular markers of cancer, Nat. Rev. Cancer 2 (3) (2002) 210–219, https://doi.org/10.1038/nrc755.
[3] N.X. Cawley, W.C. Wetsel, S.R. Murthy, J.J. Park, K. Pacak, Y.P. Loh, New roles of carboxypeptidase E in endocrine and neural function and cancer, Endocr. Rev. 33 (2) (2012) 216–253, https://doi.org/10.1210/er.2011-1039.
[4] C. Hall, E. Manser, N.K. Spurr, L. Lim, Assignment of the human carboxypeptidase E (CPE) gene to chromosome 4, Genomics 15 (2) (1993) 461–463, https://doi.org/10.1006/geno.1993.1093.
[5] L.D. Fricker, Carboxypeptidase E and the identification of novel neuropeptides as potential therapeutic targets, Adv. Pharmacol. 82 (2018) 85–102, https://doi.org/10.1016/bs.apha.2017.09.001.
[6] V.Y. Hook, L.E. Eiden, M.J. Brownstein, A carboxypeptidase processing enzyme for enkephalin precursors, Nature 295 (5847) (1982) 341–342, https://doi.org/10.1038/295341a0.
[7] Truncating Homozygous Mutation of Carboxypeptidase E (CPE) in a Morbidly Obese Female with Type 2 Diabetes Mellitus, Intellectual Disability and Hypogonadotrophic Hypogonadism, 10.1371/journal.pone.0131417.
[8] N.X. Cawley, T. Yanik, A. Woronowicz, W. Chang, J.C. Marini, Y.P. Loh, Obese carboxypeptidase E knockout mice exhibit multiple defects in peptide hormone processing contributing to low bone mineral density, Am. J. Physiol. Endocrinol. Metab. 299 (2) (2010) E189–E197, https://doi.org/10.1152/ajpendo.00516.2009.
[9] Y. Cheng, R.M. Rodriguiz, S.R. Murthy, V. Senatorov, E. Thouennon, N.X. Cawley, D.K. Aryal, S. Ahn, B. Lecka-Czernik, W.C. Wetsel, Y.P. Loh, Neurotrophic factor-alpha1 prevents stress-induced depression through enhancement of neurogenesis and is activated by rosiglitazone, Mol. Psychiatr. 20 (6) (2015) 744–754, https://doi.org/10.1038/mp.2014.136.
[10] A. Chougule, V. Kolli, S. Baroi, N. Ebraheim, P.J. Czernik, Y.P. Loh, B. Lecka-Czernik, Nonenzymatic and trophic activities of carboxypeptidase E regulate bone mass and bioenergetics of skeletal stem cells in mice, JBMR Plus 4 (9) (2020) e10392, https://doi.org/10.1002/jbm4.10392.
[11] S. Hareendran, X. Yang, V.K. Sharma, Y.P. Loh, Carboxypeptidase E and its splice variants: Key regulators of growth and metastasis in multiple cancer types, Cancer Lett. 548 (2022) 215882, https://doi.org/10.1016/j.canlet.2022.215882.
[12] H. Shen, J. Tan, J. Shang, M. Hou, J. Liu, L. He, S. Yao, S. He, CPE overexpression is correlated with pelvic lymph node metastasis and poor prognosis in patients with early-stage cervical cancer, Arch. Gynecol. Obstet. 294 (2) (2016) 333–342, https://doi.org/10.1007/s00404-015-3985-6.
[13] S. Supiot, W. Gouraud, L. Campion, P. Jezequel, B. Buecher, J. Charrier, M. Heymann, M. Mahe, E. Rio, M. Cherel, Early dynamic transcriptomic changes during preoperative radiotherapy in patients with rectal cancer: a feasibility study, World J. Gastroenterol. 19 (21) (2013) 3249–3254, https://doi.org/10.3748/wjg.v19.i21.3249.
[14] K. Zhou, H. Liang, Y. Liu, C. Yang, P. Liu, X. Jiang, Overexpression of CPE-ΔN predicts poor prognosis in colorectal cancer patients, Tumor Biol. 34 (6) (2013) 3691–3699, https://doi.org/10.1007/s13277-013-0952-3.
[15] A. Bhattacharjee, W.G. Richards, J. Staunton, C. Li, S. Monti, P. Vasa, C. Ladd, J. Beheshti, R. Bueno, M. Gillette, M. Loda, G. Weber, E.J. Mark, E.S. Lander, W. Wong, B.E. Johnson, T.R. Golub, D.J. Sugarbaker, M. Meyerson, Classification of human lung carcinomas by mRNA expression profiling reveals distinct adenocarcinoma subclasses, Proc. Natl. Acad. Sci. U. S. A. 98 (24) (2001) 13790–13795, https://doi.org/10.1073/pnas.191502998.
[16] I. Kuo, D. Liu, W. Lai, Y. Wang, Y.P. Loh, Carboxypeptidase E mRNA: overexpression predicts recurrence and death in lung adenocarcinoma cancer patients, Cancer Biomark 33 (3) (2022) 369–377, https://doi.org/10.3233/CBM-210206.
[17] X.H. Liang, L.L. Li, G.G. Wu, Y.C. Xie, G.X. Zhang, W. Chen, H.F. Yang, Q.L. Liu, W.H. Li, W.G. He, Y.N. Huang, X.C. Zeng, Upregulation of CPE promotes cell proliferation and tumorigenicity in colorectal cancer, BMC Cancer 13 (2013) 412, https://doi.org/10.1186/1471-2407-13-412.

[18] S. Murthy, E. Dupart, N. Al-Sweel, A. Chen, N.X. Cawley, Y.P. Loh, Carboxypeptidase E promotes cancer cell survival, but inhibits migration and invasion, Cancer Lett. 341 (2) (2013) 204–213, https://doi.org/10.1016/j.canlet.2013.08.011.

[19] A. Liu, C. Shao, G. Jin, R. Liu, J. Hao, Z. Shao, Q. Liu, X. Hu, Downregulation of CPE regulates cell proliferation and chemosensitivity in pancreatic cancer, TUMOR BIOLOGY 35 (12) (2014) 12459–12465, https://doi.org/10.1007/s13277-014-2564-y.

[20] H. Lou, Y.P. Loh, Silencing of Carboxypeptidase E expression inhibits proliferation and invasion of Panc-1 pancreatic cancer cells, F1000Res 10 (2021) 489, https://doi.org/10.12688/f1000research.53737.2.

[21] S. Fan, X. Li, L. Li, L. Wang, Z. Du, Y. Yang, J. Zhao, Y. Li, Silencing of carboxypeptidase E inhibits cell proliferation, tumorigenicity, and metastasis of osteosarcoma cells, OncoTargets Ther. 9 (2016) 2795–2803, https://doi.org/10.2147/OTT.S98991.

[22] A. Armento, E.I. Ilina, T. Kaoma, A. Muller, L. Vallar, S.P. Niclou, M.A. Krueger, M. Mittelbronn, U. Naumann, Carboxypeptidase E transmits its anti-migratory function in glioma cells via transcriptional regulation of cell architecture and motility regulating factors, Int. J. Oncol. 51 (2) (2017) 702–714, https://doi.org/10.3892/ijo.2017.4051.

[23] E. Hoering, P.N. Harter, J. Seznec, J. Schittenhelm, H. Buehring, S. Bhattacharyya, E. von Hattingen, C. Zachskorn, M. Mittelbronn, U. Naumann, The "go or grow" potential of gliomas is linked to the neuropeptide processing enzyme carboxypeptidase E and mediated by metabolic stress, Acta Neuropathol. 124 (1) (2012) 83–97, https://doi.org/10.1007/s00401-011-0940-x.

[24] E.I. Ilina, A. Armento, L.G. Sanchez, M. Reichlmeir, Y. Braun, C. Penski, D. Capper, F. Sahm, L. Jennewein, P.N. Harter, S. Zukunft, I. Fleming, D. Schulte, F. Le Guerroué, C. Behrends, M.W. Ronellenfitsch, U. Naumann, M. Mittelbronn, Effects of soluble CPE on glioma cell migration are associated with mTOR activation and enhanced glucose flux, Oncotarget 8 (40) (2017) 67567–67591, https://doi.org/10.18632/oncotarget.18747.

[25] W. Shen, Z. Song, X. Zhong, M. Huang, D. Shen, P. Gao, X. Qian, M. Wang, X. He, T. Wang, S. Li, X. Song, Sangerbox: a comprehensive, interaction-friendly clinical bioinformatics analysis platform, iMeta 1 (3) (2022) e36, https://doi.org/10.1002/imt2.36.

[26] T. Li, J. Fan, B. Wang, N. Traugh, Q. Chen, J.S. Liu, B. Li, X.S. Liu, TIMER: a web server for comprehensive analysis of tumor-infiltrating immune cells, Cancer Res. 77 (21) (2017) e108–e110, https://doi.org/10.1158/0008-5472.CAN-17-0307.

[27] J. Liu, T. Lichtenberg, K.A. Hoadley, L.M. Poisson, A.J. Lazar, A.D. Cherniack, A.J. Kovatich, C.C. Benz, D.A. Levine, A.V. Lee, L. Omberg, D.M. Wolf, C. D. Shriver, V. Thorsson, H. Hu, An integrated TCGA pan-cancer clinical data resource to drive high-quality survival outcome analytics, Cell 173 (2) (2018) 400–416, https://doi.org/10.1016/j.cell.2018.02.052.

[28] Z. Tang, C. Li, B. Kang, G. Gao, C. Li, Z. Zhang, GEPIA: a web server for cancer and normal gene expression profiling and interactive analyses, Nucleic Acids Res. 45 (W1) (2017) W98–W102, https://doi.org/10.1093/nar/gkx247.

[29] M. Franz, H. Rodriguez, C. Lopes, K. Zuberi, J. Montojo, G.D. Bader, Q. Morris, GeneMANIA update 2018, Nucleic Acids Res. 46 (W1) (2018) W60–W64, https://doi.org/10.1093/nar/gky311.

[30] K. Yoshihara, M. Shahmoradgoli, E. Martinez, R. Vegesna, H. Kim, W. Torres-Garcia, V. Trevino, H. Shen, P.W. Laird, D.A. Levine, S.L. Carter, G. Getz, K. Stemke-Hale, G.B. Mills, R.G. Verhaak, Inferring tumour purity and stromal and immune cell admixture from expression data, Nat. Commun. 4 (2013) 2612, https://doi.org/10.1038/ncomms3612.

[31] D. Zeng, Z. Ye, R. Shen, G. Yu, J. Wu, Y. Xiong, R. Zhou, W. Qiu, N. Huang, L. Sun, X. Li, J. Bin, Y. Liao, M. Shi, W. Liao, IOBR: multi-omics immuno-oncology biological research to decode tumor microenvironment and signatures, Front. Immunol. 12 (2021) 687975, https://doi.org/10.3389/fimmu.2021.687975.

[32] J. Racle, K. de Jonge, P. Baumgaertner, D.E. Speiser, D. Gfeller, Simultaneous enumeration of cancer and immune cell types from bulk tumor gene expression data, Elife 6 (2017), https://doi.org/10.7554/eLife.26476.

[33] F. Finotello, C. Mayer, C. Plattner, G. Laschober, D. Rieder, H. Hackl, A. Krogsdam, Z. Loncova, W. Posch, D. Wilflingseder, S. Sopper, M. Ijsselsteijn, T. P. Brouwer, D. Johnson, Y. Xu, Y. Wang, M.E. Sanders, M.V. Estrada, P. Ericsson-Gonzalez, P. Charoentong, J. Balko, N. de Miranda, Z. Trajanoski, Molecular and pharmacological modulators of the tumor immune contexture revealed by deconvolution of RNA-seq data, Genome Med. 11 (1) (2019) 34, https://doi.org/10.1186/s13073-019-0638-6.

[34] H. Mirzaei, S. Khataminfar, S. Mohammadparast, S.S. Sales, M. Maftouh, M. Mohammadi, M. Simonian, S.M. Parizadeh, S.M. Hassanian, A. Avan, Circulating microRNAs as potential diagnostic biomarkers and therapeutic targets in gastric cancer: current status and future perspectives, Curr. Med. Chem. 23 (36) (2016) 4135–4150, https://doi.org/10.2174/0929867323666160818093854.

[35] M. Simonian, M. Mosallayi, H. Mirzaei, Circulating miR-21 as novel biomarker in gastric cancer: diagnostic and prognostic biomarker, J. Canc. Res. Ther. 14 (2) (2018) 475, https://doi.org/10.4103/0973-1482.175428.

[36] S. Hareendran, B. Albraidy, X. Yang, A. Liu, A. Breggia, C.C. Chen, Y.P. Loh, Exosomal carboxypeptidase E (CPE) and CPE-shRNA-loaded exosomes regulate metastatic phenotype of tumor cells, Int. J. Mol. Sci. 23 (6) (2022) 3113, https://doi.org/10.3390/ijms23063113.

[37] H. Lou, Y.P. Loh, Silencing of Carboxypeptidase E expression inhibits proliferation and invasion of Panc-1 pancreatic cancer cells, F1000Research 10 (2021) 489, https://doi.org/10.12688/f1000research.53737.1.

[38] S.R.K. Murthy, E. Dupart, N. Al-Sweel, A. Chen, N.X. Cawley, Y.P. Loh, Carboxypeptidase E promotes cancer cell survival, but inhibits migration and invasion, Cancer Lett. 341 (2) (2013) 204–213, https://doi.org/10.1016/j.canlet.2013.08.011.

[39] S. Hareendran, X. Yang, V.K. Sharma, Y.P. Loh, Carboxypeptidase E and its splice variants: Key regulators of growth and metastasis in multiple cancer types, Cancer Lett. 548 (2022) 215882, https://doi.org/10.1016/j.canlet.2022.215882.

[40] Z. Bai, M. Feng, Y. Du, L. Cong, Y. Cheng, Carboxypeptidase E down-regulation regulates transcriptional and epigenetic profiles in pancreatic cancer cell line: a network analysis, Cancer Biomark 29 (1) (2020) 79–88, https://doi.org/10.3233/CBM-191163.

[41] N. Landeros, P.M. Santoro, G. Carrasco-Avino, A.H. Corvalan, Competing endogenous RNA networks in the epithelial to mesenchymal transition in diffuse-type of gastric cancer, Cancers 12 (10) (2020), https://doi.org/10.3390/cancers12102741.

[42] Z. Peng, C.X. Wang, E.H. Fang, G.B. Wang, Q. Tong, Role of epithelial-mesenchymal transition in gastric cancer initiation and progression, World J. Gastroenterol. 20 (18) (2014) 5403–5410, https://doi.org/10.3748/wjg.v20.i18.5403.

[43] B. Yue, C. Song, L. Yang, R. Cui, X. Cheng, Z. Zhang, G. Zhao, METTL3-mediated N6-methyladenosine modification is critical for epithelial-mesenchymal transition and metastasis of gastric cancer, Mol. Cancer 18 (1) (2019) 142, https://doi.org/10.1186/s12943-019-1065-4.

[44] K.T. Yeung, J. Yang, Epithelial-mesenchymal transition in tumor metastasis, Mol. Oncol. 11 (1) (2017) 28–39, https://doi.org/10.1002/1878-0261.12017.

[45] K. Liu, K. Yang, B. Wu, H. Chen, X. Chen, X. Chen, L. Jiang, F. Ye, D. He, Z. Lu, L. Xue, W. Zhang, Q. Li, Z. Zhou, X. Mo, J. Hu, Tumor-infiltrating immune cells are associated with prognosis of gastric cancer, Medicine (Baltim.) 94 (39) (2015) e1631, https://doi.org/10.1097/MD.0000000000001631.

[46] J. Zhou, Z. Tang, S. Gao, C. Li, Y. Feng, X. Zhou, Tumor-associated macrophages: recent insights and therapies, Front. Oncol. 10 (2020) 188, https://doi.org/10.3389/fonc.2020.00188.

[47] Y. Yan, J. Zhang, J.H. Li, X. Liu, J.Z. Wang, H.Y. Qu, J.S. Wang, X.Y. Duan, High tumor-associated macrophages infiltration is associated with poor prognosis and may contribute to the phenomenon of epithelial-mesenchymal transition in gastric cancer, OncoTargets Ther. 9 (2016) 3975–3983, https://doi.org/10.2147/OTT.S103112.

[48] C. Su, S. Jia, H. Liu, Immunolocalization of CD163+ tumor-associated macrophages and symmetric proliferation of ki-67 as biomarkers to differentiate new different grades of laryngeal dysplasia, Am. J. Clin. Pathol. 149 (1) (2017) 8–16, https://doi.org/10.1093/ajcp/aqx107.

[49] G. Sammarco, C.D. Gadaleta, V. Zuccala, E. Albayrak, R. Patruno, P. Milella, R. Sacco, M. Ammendola, G. Ranieri, Tumor-associated macrophages and mast cells positive to tryptase are correlated with angiogenesis in surgically-treated gastric cancer patients, Int. J. Mol. Sci. 19 (4) (2018), https://doi.org/10.3390/ijms19041176.

[50] D. Zhang, X. Qiu, J. Li, S. Zheng, L. Li, H. Zhao, TGF-beta secreted by tumor-associated macrophages promotes proliferation and invasion of colorectal cancer via miR-34a-VEGF axis, Cell Cycle 17 (24) (2018) 2766–2778, https://doi.org/10.1080/15384101.2018.1556064.

[51] W. Song, R. Mazzieri, T. Yang, G.C. Gobe, Translational significance for tumor metastasis of tumor-associated macrophages and epithelial-mesenchymal transition, Front. Immunol. 8 (2017) 1106, https://doi.org/10.3389/fimmu.2017.01106.